Importance of the Hydrogen Isocyanide Isomer in Modeling Hydrogen Cyanide Oxidation in Combustion

Glarborg, Peter; Marshall, Paul

Published in:
Energy & Fuels

Link to article, DOI:
10.1021/acs.energyfuels.6b02085

Publication date:
2017

Document Version
Peer reviewed version

Importance of the HNC isomer in modeling HCN oxidation in combustion

Peter Glarborg*,† and Paul Marshall‡

†*DTU Chemical Engineering, Technical University of Denmark, 2800 Lyngby, Denmark*

‡*Department of Chemistry and Center for Advanced Scientific Computing and Modeling (CASCaM), University of North Texas, Denton, 1155 Union Circle #305070, Texas 76203–5017*

E-mail: pgl@kt.dtu.dk

Hydrogen isocyanide (HNC) has been proposed as an important intermediate in oxidation of HCN in combustion, but details of its chemistry are still in discussion. At higher temperatures, HCN and HNC equilibrate rapidly, and being more reactive than HCN, HNC offers a fast alternative route of oxidation for cyanides. However, in previous modeling it has been required to omit the HNC subset partly or fully in the reaction mechanisms to obtain satisfactory predictions. In the present work, we re-examine the chemistry of HNC and its role in combustion nitrogen chemistry. The HNC + O_2 reaction is studied by ab initio methods and is shown to have a high barrier. Consequently, the omission of this reaction in recent modeling studies is justified. With the present knowledge of the HNC chemistry, including an accurate value of the heat of formation for HNC and improved rate constants for HNC + O_2 and HNC + OH, it is possible to reconcile the modeling issues and provide a satisfactory prediction of a wide range of experimental results on HCN oxidation. In the burned gases of fuel-rich flames where HCN and CN are partially equilibrated and the sequence HCN $\xrightarrow{+M}$ HNC $\xrightarrow{+OH}$ HNCO is the major consumption path for HCN. Under lean conditions HNC is

shown to be less important than indicated by the early work by Lin and coworkers, but it acts to accelerate HCN oxidation and promotes formation of HNCO.

Introduction

In combustion processes, cyanides may be formed from devolatilization of fuels with organically bound nitrogen, from reaction of hydrocarbon radicals (CH, C) with N_2 (the initiating step in prompt NO formation), from reaction of reactive nitrogen species such as NO or amines with hydrocarbon radicals, or from decomposition of hydrocarbon amines.[1–5] In sufficiently fuel-rich hydrocarbon flames it appears that hydrogen cyanide (HCN) is the dominant nitrogenous species leaving the primary reaction zone, regardless of the source of the nitrogen,[6–8] and it is considered the predominant cyanide species in combustion. The oxidation chemistry of HCN has been studied extensively over the years. Much of this work was reviewed recently by Dagaut et al.[9]

An unresolved issue in the oxidation chemistry of HCN is the role of its isomer, hydrogen isocyanide (HNC). As suggested initially by Lin et al.,[10] isomerization of HCN to HNC, followed by oxidation of HNC, represents an alternative pathway for HCN oxidation. The reactivity of HNC is quite different from that of HCN and presence of HNC in significant quantities may affect the oxidation behavior of hydrogen cyanide. Hydrogen isocyanide is formed by isomerization of HCN,

$$\mathrm{HCN + M \rightleftharpoons HNC + M} \qquad \text{(R2)}$$

or by an H-atom exchange reaction of HCN with H,

$$\mathrm{HCN + H \rightleftharpoons HNC + H} \qquad \text{(R12b)}$$

At high temperatures these reactions lead to fast equilibration of HNC with HCN. Once

formed, HNC has been proposed to react rapidly with OH and O_2,[11]

$$HNC + OH \rightleftharpoons HNCO + H \tag{R14}$$

$$HNC + O_2 \rightleftharpoons HNCO + O \tag{R16a}$$

$$HNC + O_2 \rightleftharpoons NH + CO_2 \tag{R16b}$$

Since these steps are presumably much faster than the corresponding reactions of HCN with OH and O_2, they serve to enhance the consumption rate of HCN and convert the cyanide pool to isocyanide species and amines. According to Dagaut et al.,[9] the impact of HNC on HCN consumption is most pronounced for the conditions in shock tubes and flow reactor systems, while it is less important in laminar premixed flames. However, inclusion of a kinetic subset for HNC with the accepted thermochemistry for this species and rate constants for HNC reactions drawn from the evaluation of Dean and Bozzelli[11] leads to a considerable reduction in the accuracy of modeling predictions when compared to experimental data.[9] To obtain acceptable modeling accuracy, Dagaut et al.[9] omitted HNC + O_2 (R16) from their reaction mechanism; otherwise predicted ignition delays for HCN under shock tube conditions were too low by an order of magnitude. Dagaut et al. concluded in their review that further work was needed to assess the kinetics of HNC reactions, in particular that of HNC + O_2. This suggestion was supported by Gimenez-Lopez et al.[12] in a recent flow reactor study on HCN oxidation in a CO_2/N_2 atmosphere, where they found inclusion of the HNC + O_2 reaction to lead to overprediction of the HCN consumption rate.

While the importance of HNC in combustion systems has attracted only modest interest,[9–11,13,14] the properties of hydrogen isocyanide have been studied extensively[15–67] due in part to its small size, which allows for study at high levels of theory, and in part to its potential importance in astrochemistry. The objective of the present work is to re-evaluate the HNC chemistry, with particular emphasis on HNC + O_2 which is studied by ab initio methods, and assess the implications for modeling HCN oxidation in combustion.

Detailed Kinetic Model and Ab Initio Calculations

The cyanide subset of the chemical kinetic model was based on the work of Dagaut et al.[9] In the present study, the thermochemistry of HNC, as well as rate constants for the reactions involved in forming or consuming HNC, was re-evaluated. In addition, the hydrogen and amine chemistry subsets were updated based on recent work.[5,68–75] The full model is available as supplementary material.

The thermodynamic properties of HNC are important, since they determine the HNC/HCN ratio at high temperatures where the two isomers equilibrate rapidly. Table 1 summarizes the values reported in the literature for the heat of formation of HNC and the energy difference between HNC and HCN. The early experimental determinations of the energy separation between the isomers range from 10.3 kcal mol^{-1} [22] to more than 17 kcal mol^{-1},[23] but more recent work serves to reduce the uncertainty. Most theoretical predictions[15,20,32,34,35,38,42,46,52,62,67] support a value for ΔH^0_{f298}(HNC) - ΔH^0_{f298}(HCN) of 14.2-15.3 kcal mol^{-1}, in agreement with the experimental value of 14.8 kcal mol^{-1} from Pau and Hehre.[24]

The Pau and Hehre results were questioned by Wenthold[45] based on revisions in the proton affinity scale in later years. From experimental work, as well as a reinterpretation of the results of Pau and Hehre, Wenthold obtained a value for the heat of formation of HNC of ΔH^0_{f298}(HNC) = 49.7±2.9 kcal mol^{-1}, corresponding to an energy difference between HNC and HCN of 18.8±2.9 kcal mol^{-1}. A high value was also obtained recently by Barber et al.[61] from a high-level multireference configuration interaction study. They found an energy difference between HNC and HCN of 16.3 kcal mol^{-1}, corresponding to a heat of formation for HNC of 47.2 kcal mol^{-1}.

The high values of ΔH^0_{f298}(HNC) determined by Wenthold[45] and Barber et al.[61] would diminish the importance of HNC in combustion modeling. However, they are called into question in the recent study by Nguyen et al.[67] who investigated the HCN → HNC 0 K isomerization energy by combining state-of-the-art electronic structure methods with the Active Thermochemical Tables (ATcT) approach. They found the energy difference between

HCN and HNC at 298 K to be 15.1 kcal mol^{-1}. This is substantially lower than the values of Barber et al. and Wenthold (by 1.2 and 3.7 kcal mol^{-1}, respectively). Nguyen et al. concluded that the value from Barber et al. was likely to have a much larger uncertainty than originally stated. The analysis from Nguyen et al. indicates that the heat of formation of HNC at 298 K is 45.95±0.09 kcal mol^{-1}; we have adopted this value in the present work. An energy separation between HNC and HCN of 15.1 kcal mol^{-1} is 2.2 kcal mol^{-1} higher than that used in the early study by Lin et al.[10] and adopted by Dean and Bozzelli[11] and recently by Lamoureux et al.[14], and 0.3 kcal mol^{-1} higher than the recommendation of Dagaut et al.[9].

Table 2 lists thermodynamic properties for HNC, HCN and CN. The thermodynamic properties in the present work were generally adopted from the Ideal Gas Thermochemical Database by Goos, Burcat and Ruscic,[78] with properties obtained using the Active Thermochemical Tables (ATcT) approach.[79,80]

Table 3 lists key reactions of HCN and HNC from the chemical kinetic model. There are no reported experimental studies of HNC reactions and rate constants have been obtained from theory. However, from the available theoretical studies it is obvious that the reactivity of HNC is quite different from that of HCN. HNC can be formed by isomerization of HCN,

$$\mathrm{HCN + M \rightleftharpoons HNC + M} \qquad \text{(R2)}$$

or by reaction of HCN with H,

$$\mathrm{HCN + H \rightleftharpoons HNC + H} \qquad \text{(R12b)}$$

The isomerization step has been studied extensively by theory.[10,11,32,34,35,38,42,49,52,53,64] Estimates of the barrier for the isomerization range from 44.7 to 48.2 kcal mol^{-1}.[10,11,32,34,35,38,42] With a barrier of this magnitude, isomerization (R2) is much faster than thermal dissociation of HCN (R1), and HCN will isomerize fairly easily to HNC at medium to high temperatures. Following Dagaut et al.,[9] we have adopted the rate constant for (R2) from the evaluation of

Dean and Bozzelli,[11] but modified the activation energy to reflect the larger energy separation between HCN and HNC. Also reaction (R12b) has been studied theoretically,[85,87]; we have included this step in the exothermic direction, HNC + H $\rightleftharpoons$ HCN + H (R12), with a rate constant calculated by Sumathi and Nguyen.[85]

The most important consumption reaction of HNC is presumably HNC + OH,

$$\mathrm{HNC + OH \rightleftharpoons HNCO + H} \tag{R14}$$

Figure 1 shows an Arrhenius plot for the reaction. In their early evaluation, Lin et al.[10] calculated an activation energy for (R14) of 3.7 kcal mol^{-1}. Recently, the reaction was studied at a high level of theory by Bunkan et al.[86] for the 250-350 K range. They predict the rate constant to have a slight negative temperature dependence, at least at low temperatures. Their reaction path shows a pre-reaction complex followed by a transition state (TS) whose energy is $\sim$ 1.1 kcal mol^{-1} below that of the reactants. Their RRKM kinetic analysis should correctly allow for the lack of population of energy levels of the TS below the reactants at modest pressures. Based on a recomputation of the unpublished CCSD(T) frequencies of the TS, we have made a preliminary assessment of the high pressure limit via transition state theory. This calculation indicates that $k_{14,\infty}$ may reach a minimum and then increase at higher temperatures. However, more work is required to calculate accurately the effect of temperature and pressure on this reaction. In the current work, we have extrapolated directly the results from Bunkan et al. to higher temperatures with a small negative activation energy (Fig. 1) fitted to the published k_{14} values.

For the possible other product channel,

$$\mathrm{HNC + OH \rightleftharpoons CN + H_2O} \tag{R15}$$

Bunkan et al. deduced a barrier of more than 16 kcal mol^{-1}, which makes that channel too slow to compete under atmospheric conditions. Combination of their barrier with M06-

2X/6-311+G(3df,2p) vibrational frequencies and geometry for the TS leads to a predicted rate constant of $3.0 \cdot 10^2$ $T^{3.16}$ exp(-5330/T) cm^3 mol^{-1} s^{-1} over 600-3000 K. Tunneling makes a major contribution so there is considerable uncertainty in this expression, perhaps an order of magnitude at the lower end of the temperature range.

For the reaction of HNC with O,

$$HNC + O \rightleftharpoons NH + CO \tag{R13}$$

we adopt the rate constant proposed by Lin et al.[10] from a combined experimental and theoretical study. Unfortunately the experimental results referred to by Lin et al. were never published, and more work on this step is desirable.

Dean and Bozzelli suggested that oxygen could readily add to HNC and that subsequent isomerization or dissociation steps would lead to HNCO + O and NH + CO_2,[11]

$$HNC + O_2 \rightleftharpoons HNCO + O \tag{R16a}$$

$$HNC + O_2 \rightleftharpoons NH + CO_2 \tag{R16b}$$

They computed low barriers for both channels and obtained rate constants of $k_{16a} = 1.5 \times 10^{12}$ $T^{0.01}$ exp(-2068/T) cm^3 mol^{-1} s^{-1} and $k_{16b} = 1.6 \times 10^{19}$ $T^{-2.25}$ exp(-896/T) cm^3 mol^{-1} s^{-1}. However, Dagaut et al.,[9] found it necessary to omit the HNC+O_2 reaction in their modeling study to obtain consistency with experimental results. More recently Gimenez-Lopez et al.[12] and Lamoreux et al.[14] also disregarded HNC+O_2 in their reaction mechanisms. This prompted us to characterize the reaction by ab initio methods.

We find that a triplet HNCOO adduct lies ca. 42 kcal mol^{-1} above HNC + O_2 at the CBS-QB3 level of theory, and the barrier to forming this adduct (including zero-point energy) is even higher, at about 44 kcal mol^{-1} which is confirmed by CCSD(T)/cc-pVTZ calculations.[88,89] The high energy barrier makes the reaction insignificant under most conditions of

interest. Singlet HNCOO is even less stable.

The reaction of HCN with OH is of particular interest in this work, as it competes directly with HNC + OH (R14). It is a complicated step, involving multiple potential wells and multiple product channels[1],

$$HCN + OH \rightleftharpoons CN + H_2O \quad \text{(R7)}$$

$$HCN + OH \rightleftharpoons HOCN + H \quad \text{(R8)}$$

$$HCN + OH \rightleftharpoons HNCO + H \quad \text{(R9)}$$

$$HCN + OH \rightleftharpoons NH_2 + CO \quad \text{(R10)}$$

The rate constant for H-abstraction channel to form CN + H_2O (R7) has been measured directly both in the forward and reverse direction. Figure 2 shows an Arrhenius plot for this step. Wooldridge et al.[83] determined k_7 from CN and OH time histories in shock tube experiments. The results shown from Jacobs et al.[90] were obtained for the reverse reaction and have been converted using the present thermodynamic properties for the involved species. The two data sets are in very good agreement, indicating that the rate constant for this reaction is known quite accurately. The experiments of Wooldridge et al. are analyzed further below.

For the other product channels of HCN + OH (R8-R10), rate constants are drawn from BAC-MP4 calculations by Miller and Melius[84]. There are no experimental data for these product channels, and more work is desirable to support the rate constants. At most conditions the H-abstraction reaction (R7) dominates, but at very low temperatures formation of HNCO + H (R9) is competitive, while at temperatures above 2000 K HOCN + H (R8) becomes the fastest channel.

Results and Discussion

This section aims to clarify the role of HNC in oxidation of HCN at medium to high temperatures relevant for combustion. Hydrogen cyanide is presumably the most important precursor of HNC in combustion, and the expected role of HNC is to accelerate the HCN consumption, converting it to isocyanides and amines.

Haynes[8] investigated the decay of hydrogen cyanide in the burnt gases of a number of fuel-rich, atmospheric pressure hydrocarbon flames. Independent of the type of nitrogen additive (ammonia or pyridine), it was converted to HCN in the reaction zone of the flame, with smaller amounts of NO. In the post-flame zone, HCN was slowly converted to NH_3. Haynes found the decay mechanism for HCN at temperatures below 2300 K to be first order in OH, and he assumed it to be

$$HCN + OH \rightarrow (HOCN) + H$$

or a kinetically equivalent process, with the (HOCN) isomer eventually converted to NH_3.

Figure 3 compares Haynes' measurements for a rich ethylene flame doped with ammonia with modeling predictions. The temperature of the burnt gases was 2000 K. In the modeling, only the post-flame zone was considered. It was assumed that both acetylene and oxygen were depleted in the reaction zone, resulting in an equilibrium mixture of CO, H_2, CO_2, and H_2O entering the post-flame zone. In the calculations, the equilibrium composition at 2000 K, together with the measured concentrations of HCN, NH_3, and NO, was used as the inlet composition. The modeling predictions (solid lines) are in good agreement with the measurements for HCN, NH_3, and NO. Analysis of the present calculations indicates that HCN consumed through a two step sequence,

$$HCN + M \rightleftharpoons HNC + M \qquad \text{(R2)}$$

$$HNC + OH \rightarrow HNCO + H \qquad \text{(R14)}$$

This sequence is kinetically equivalent to the reaction proposed by Haynes. Under the conditions in the flame, HCN equilibrates rapidly with HNC. Atomic hydrogen and to a lesser extent OH are the dominant radicals in the flame but they consume little HCN because the reactions HCN + H $\rightleftharpoons$ CN + H_2 (R3b) and HCN + OH $\rightleftharpoons$ CN + H_2O (R7) are both rapidly equilibrated. This makes the conditions favorable to study the reactions of HNC, in particular HNC + OH (R14), even though other product channels for HCN + OH, in particular (R8), are also active. The HNCO formed in (R14) feeds rapidly into the amine pool, eventually forming NH_3:

$$HNCO + H \rightleftharpoons NH_2 + CO$$

$$NH_2 + H_2 \rightleftharpoons NH_3 + H$$

A smaller fraction of the NH_2 is converted to NH and N through the sequence $NH_2 \xrightarrow{+H}$ NH $\xrightarrow{+H}$ N. The NH and N radicals may be oxidized to NO by reaction with OH or react with NO to form N_2O or N_2. This competition results overall in a small decrease in NO concentration.

In Fig. 3, dashed lines show predictions with the rate constant for HNC + OH (R14) varied by a factor of two. The results show that the predicted HCN and NH_3 profiles are quite sensitive to the value of k_{14}. This is confirmed by Fig. 4, which shows the results of a sensitivity analysis for HCN and NH_3 for the conditions of Fig. 3. For HCN, the rate constant for (R14) has by far the largest sensitivity coefficient. Also the predicted NH_3 concentration is sensitive mostly to this step. The good agreement obtained in modeling for both of these species support the accuracy of k_{14} at this temperature. The OH radical maintains a partial equilibrium in the post-flame reqion and modeling predictions are not sensitive to chain branching or terminating steps.

For high temperature conditions in a shock tube, the isomerization of HCN to HNC is suf-

ficiently rapid to occur at the same μs time scale as the observed chemistry,[11] and predicted induction times for HCN/O_2 mixtures are quite sensitive to the HNC subset.[9] Higashihara et al.[91] studied the oxidation of HCN by O_2 in a shock tube over the temperature range 1450-2600 K and pressures of 0.75-2.0 atm. They measured the UV signal from electronically excited OH and defined the induction time τ_{OH*} as the time where the UV emission started to increase rapidly. OH* was assumed to be formed largely from recombination of O and H radicals. For the HCN/O_2 system the OH* induction time from a least-square analysis could be represented as $\tau_{OH*} = 10^{-13.42}$ exp(-12200/T) $[HCN]^{-0.44}$ $[O_2]^{-0.17}$ $[Ar]^{-0.52}$ s.

In Fig. 5, data estimated from this empirical expression are compared to predictions using the chemical kinetic model. In this figure, as well as in the following, modeling predictions are shown for three different mechanisms:

1. The full present mechanism.

2. The present mechanism excluding the HNC subset.

3. The present mechanism with ΔH^0_{f298}(HNC) - ΔH^0_{f298}(HCN) = 12.9 kcal mol^{-1} [10,11,14], and rate constants from Dean and Bozzelli[11], including the HNC + O_2 reaction.

In the modeling of the data in Fig. 5, the OH* induction time is defined as the time to reach 25% of the peak concentration of O. Predictions with the present model with (solid line) and without (short-dashed line) the HNC subset are both in good agreement with the measured induction times. The similarity between predictions with and without HNC indicates that this species, with the present chemistry, plays only a small role under these conditions. However, if the HNC subset is replaced by that recommended by Dean and Bozzelli,[11] the predicted induction time is lowered by more than a factor of 10, in conflict with the experimental observations. The too low value for the energy separation between HNC and HCN contributes to the discrepancy, because it leads to overprediction of the HNC

concentration. However, most of the difference is caused by the fast rate constants for HNC + O_2 estimated by Dean and Bozzelli.

Wooldridge et al.[83] measured CN and OH time histories in incident and reflected shock waves using dilute mixtures of HCN and nitric acid (HNO_3) in argon. The thermal decomposition of HNO_3 yielded OH upon shock-heating, and the OH subsequently reacted predominantly with HCN. As discussed above, they used the data to deduce a rate constant for the reaction HCN + OH $\rightleftharpoons$ CN + H_2O (R7). Their simultaneous measurements of CN and OH yielded values of k_7 in good agreement, putting severe limitations on the importance of the HNC isomer. Wooldridge et al. concluded that they had to omit reactions of HNC to obtain a satisfactory agreement between their observed concentration profiles and modeling results. A further constraint on HNC + OH is the excellent consistency between the two data sets from Wooldridge et al. and Jacobs et al.[90] obtained for the reverse reaction (Fig. 2). Apparently HNC + OH cannot have had a significant impact on the OH concentration profile in the experiments of Wooldridge et al.

Figure 6 shows a comparison between experimental results obtained at 1492 K and modeling predictions with the present reaction mechanism. For these conditions, Wooldridge et al. reported only the OH concentration profile; at higher temperatures, where concentrations were reported for both OH and CN, predictions are less sensitive to reactions of HNC since HCN + OH becomes more competitive. As expected, the model (solid line) is seen to overestimate the OH consumption rate. The discrepancy, which is due to OH consumption by HNC + OH (R14), can be removed by taking out HNC from the reaction mechanism (short-dashed line), as proposed by Wooldridge et al. However, we find the level of agreement to be satisfactory as it is within the 30% overall uncertainty attributed to k_7 by Wooldridge et al. due uncertainties in side reactions. As expected, predictions with the Dean and Bozzelli HNC subset (long-dashed line) shows a larger deviation, partly due the difference in thermochemistry and partly to a faster rate constant for HNC + OH.

Figure 7 compares flow reactor results from Glarborg and Miller[13] on lean HCN oxidation

with modeling predictions. The experiments were conducted at 900-1400 K and atmospheric pressure with a dilute mixture of HCN, O_2, and H_2O in N_2, and the product composition at the reactor outlet was measured. The calculations show a considerable impact of the choice of HNC subset. The preferred model provides a good agreement with the measured profiles of HCN, HNCO, and NO, while omission of the HNC subset leads to delayed onset of reaction. The Dean and Bozzelli HNC subset leads to premature ignition and a strong underprediction of HNCO.

In Fig. 8, jet-stirred reactor experiments reported by Dagaut et al.[92] for the oxidation of HCN are compared with modeling predictions. The modeling predictions agree well with the measured profiles for HCN and NO, but HNCO is underpredicted by almost a factor of two. Exclusion of the HNC subset has only a small impact on HCN and NO predictions, but acts to increase the discrepancy for HNCO. Use of the HNC subset from Dean and Bozzelli leads to a too fast calculated consumption of HCN and has an adverse impact also on the HNCO prediction.

Conclusions

The chemistry of HNC and its role in combustion nitrogen chemistry have been re-examined. The HNC + O_2 reaction was studied by ab initio methods and shown to have a high barrier. With an updated kinetic subset for the HNC chemistry, including an accurate value of the heat of formation for HNC and improved rate constants for HNC + O_2 and HNC + OH, it was possible to reconcile modeling issues and provide a satisfactory prediction of a wide range of experimental results on HCN oxidation. In the burned gases of fuel-rich flames where HCN and CN is partially equilibrated the sequence HCN $\xrightarrow{+M}$ HNC $\xrightarrow{+OH}$ HNCO is the major consumption path for HCN. Under lean conditions HNC is shown to be less important than indicated by the early work of Lin and coworkers, but it acts to accelerate HCN oxidation and promotes formation of HNCO.

Acknowledgments

The work is part of the CHEC (Combustion and Harmful Emission Control) research program. It was financially supported by the Technical University of Denmark. PM thanks the R.A. Welch Foundation (Grant B-1174) for support. PG thanks Drs. Branko Ruscic, Stephen Klippenstein, and James A. Miller for helpful discussions.

References

(1) Miller, J. A.; Bowman, C. T. *Prog. Energy Combust. Sci.* **1989**, *15*, 287–338.

(2) Bowman, C. T. *Proc Combust Inst* **1992**, *24*, 859–878.

(3) Glarborg, P.; Jensen, A. D.; Johnsson, J. E. *Prog Energy Combust Sci* **2003**, *29*, 89–113.

(4) Glarborg, P. *Proc Combust Inst* **2007**, *31*, 77–98.

(5) Lucassen, A.; Zhang, K.; Warkentin, J.; Moshammer, K.; Glarborg, P.; Marshall, P.; Kohse-Höinghaus, K. *Combust Flame* **2012**, *159*, 2254–2279.

(6) Haynes, B. S.; Iverach, D.; Kirov, N. Y. *Proc Combust Inst* **1975**, *15*, 1103–1112.

(7) Fenimore, C. P. *Combust Flame* **1976**, *26*, 249–256.

(8) Haynes, B. S. *Combust Flame* **1977**, *28*, 113–121.

(9) Dagaut, P.; Glarborg, P.; Alzueta, M. U. *Prog Combust Energy Sci* **2008**, *34*, 1–46.

(10) Lin, M. C.; He, Y.; Melius, C. F. *Int J Chem Kinet* **1992**, *24*, 1103–1107.

(11) Dean, A. M.; Bozzelli, J. W. In *Gas Phase Combustion Chemistry*; Gardiner, W. C., Ed.; Springer-Verlag, 2000; Chapter 2.

(12) Gimenez-Lopez, J.; Millera, A.; Bilbao, R.; Alzueta, M. U. *Combust Flame* **2010**, *157*, 267–276.

(13) Glarborg, P.; Miller, J. A. *Combust Flame* **1994**, *99*, 475–483.

(14) Lamoureux, N.; Merhubi, H. E.; Pillier, L.; de Persis, S.; Desgroux, P. *Combust Flame (2016)* **2016**, *163*, 557–575.

(15) Pearson, P. K.; Schaefer, H. F.; Wahlgren, U. *J Chem Phys* **1975**, *62*, 350–354.

(16) Vonniessen, W.; Cederbaum, L. S.; Domcke, W.; Diercksen, G. H. F. *Mol Phys* **1976**, *32*, 1057–1061.

(17) Ishida, K.; Morokuma, K.; Komornicki, A. *J Chem Phys* **1977**, *66*, 2153–2156.

(18) Dorschner, R.; Kaufmann, G. *Inorg Chim Acta* **1977**, *23*, 97–101.

(19) Gray, S. K.; Miller, W. H.; Yamaguchi, Y.; Schaefer, H. F. *J Chem Phys* **1980**, *73*, 2733–2739.

(20) Redmon, L. T.; Purvis, G. D.; Bartlett, R. J. *J Chem Phys* **1980**, *72*, 986–991.

(21) Vazquez, G. J.; Gouyet, J. F. *Chem Phys Lett* **1981**, *77*, 233–238.

(22) Maki, A. G.; Sams, R. L. *J Chem Phys* **1981**, *75*, 4178–4182.

(23) Maricq, M. M.; Smith, M. A.; Simpson, C. J. S. M.; Ellison, G. B. *J Chem Phys* **1981**, *74*, 6154–6170.

(24) Pau, C. F.; Hehre, W. J. *J Chem Phys* **1982**, *86*, 321–322.

(25) Peric, M.; Mladenovic, M.; Peyerimhoff, S. D.; Buenker, R. J. *J Chem Phys* **1983**, *82*, 317–336.

(26) Glidewell, C.; Thomson, C. *J Comput Chem* **1984**, *5*, 1–10.

(27) Peric, M.; Mladenovic, M.; Peyerimhoff, S. D.; Buenker, R. J. *J Chem Phys* **1984**, *86*, 85–103.

(28) Waite, B. A. *J Chem Phys* **1984**, *88*, 5076–5083.

(29) Bacic, Z.; Gerber, R. B.; Ratner, M. A. *J Chem Phys* **1986**, *90*, 3606–3612.

(30) Smith, R. S.; Shirts, R. B.; Patterson, C. W. *J Chem Phys* **1987**, *86*, 4452–4460.

(31) Szalay, V. *J Chem Phys* **1990**, *92*, 3633–3644.

(32) Lee, T. J.; Rendell, A. P. *Chem Phys Lett* **1991**, *177*, 491–497.

(33) Lan, B. L.; Bowman, J. M. *J Chem Phys* **1993**, *97*, 12535–12540.

(34) Bowman, J. M.; Gazdy, B.; Bentley, J. A.; Lee, T. J.; Dateo, C. E. *J Chem Phys* **1993**, *99*, 308–323.

(35) Gazdy, B.; Musaev, D. G.; Bowman, J. M.; Morokuma, K. *Chem Phys Lett* **1995**, *237*, 27–32.

(36) Zhao, M. S. *Chin J Chem* **1995**, *13*, 141–149.

(37) Talbi, D.; Ellinger, Y.; Herbst, E. *Astron Astrophys* **1996**, *314*, 688–692.

(38) Talbi, D.; Ellinger, Y. *Chem Phys Lett* **1996**, *263*, 385–392.

(39) Rao, V. S.; Vijay, A.; Chandra, A. K. *Can J Chem Rev Can Chim* **1996**, *74*, 1072–1077.

(40) Jursic, B. S. *J Chem Soc Faraday Trans* **1997**, *93*, 2355–2359.

(41) Bowman, J. M.; Gazdy, B. *J Phys Chem A* **1997**, *101*, 6384–6388.

(42) Contreras, R.; Safont, V. S.; Perez, P.; Moliner, J. A.; Tapia, O. *J Mol Struct (Theochem)* **1998**, *426*, 277–288.

(43) Kumeda, Y.; Minami, Y.; Takano, K.; Taketsugu, T.; Hirano, T. *J Mol Struct (Theochem)* **1999**, *458*, 285–291.

(44) Christoffel, K. M.; Bowman, J. M. *J Chem Phys* **2000**, *112*, 4496–4505.

(45) Wenthold, P. G. *J Phys Chem A* **2000**, *104*, 5612–5616.

(46) van Mourik, T.; Harris, G. J.; Polyansky, O. L.; Tennyson, J.; Csaszar, A. G.; Knowles, P. J. *J Chem Phys* **2001**, *115*, 3706–3718.

(47) Barber, R. J.; Harris, G. J.; Tennyson, J. *J Chem Phys* **2002**, *117*, 11239–11243.

(48) Liao, X. L.; Wu, W.; Mo, Y. R.; Zhang, Q. N. *Sci China Ser B Chem* **2003**, *46*, 316–370.

(49) Isaacson, A. D. *J Phys Chem A* **2006**, *110*, 379–388.

(50) Harris, G. J.; Tennyson, J.; Kaminsky, B. M.; Pavlenko, Y. V.; Jones, H. R. A. *Mon Not R Astron Soc* **2006**, *367*, 400–406.

(51) Mellau, G. C.; Winnewisser, B. P.; Winnewisser, M. *J Mol Spectrosc* **2008**, *249*, 23–42.

(52) DePrince III, A. E.; Mazziotti, D. A. *J Phys Chem B* **2008**, *112*, 16158–16162.

(53) Quapp, W.; Zech, A. *J Comput Chem* **2010**, *31*, 573–585.

(54) Mellau, G. C. *J Chem Phys* **2010**, *133*, 164303.

(55) Mellau, G. C. *J Mol Spectrosc* **2010**, *264*, 2–9.

(56) Mellau, G. C. *J Chem Phys* **2011**, *134*, 234303.

(57) Mellau, G. C. *J Mol Spectrosc* **2011**, *269*, 77–85.

(58) Mellau, G. C. *J Chem Phys* **2011**, *134*, 194302.

(59) Mellau, G. C. *J Mol Spectrosc* **2011**, *269*, 12–20.

(60) Hebrard, E.; Dobrijevic, M.; Loison, J. C.; Bergeat, A.; Hickson, K. M. *Astro Astrophys* **2012**, *541*, A21.

(61) Barber, R. J.; Strange, J. K.; Hill, C.; Polyansky, O. L.; Mellau, G. C.; Yurchenko, S. N.; Tennyson, J. *Mon Not R Astron Soc* **2014**, *437*, 1828–1835.

(62) Vichietti, R. M.; Haiduke, R. L. A. *Mon Not R Astron Soc* **2014**, *437*, 2351–2360.

(63) Loison, J. C.; Wakelam, V.; Hickson, K. M. *Mon Not R Astron Soc* **2014**, *443*, 398–410.

(64) Gutierrez-Oliva, J. S.; Diaza, S.; Toro-Labbea, A.; Laneb, P.; Murray, J. S.; Politzer, P. *Mol Phys* **2014**, *112*, 349–354.

(65) Gutierrez-Oliva, S.; Díaz, S.; Toro-Labbe, A.; Lane, P.; Murray, J. S.; Politzer, P. *Mol Phys* **2014**, *112*, 398–410.

(66) Baraban, J. H.; Changala, P. B.; Mellau, G. C.; Stanton, J. F.; Merer, A. J.; Field, R. W. *Science* **2015**, *350*, 1338–1342.

(67) Nguyen, T. L.; Baraban, J. H.; Ruscic, B.; Stanton, J. F. *J Phys Chem A* **2015**, *119*, 10929–10934.

(68) Hashemi, H.; Christensen, J. M.; Gersen, S.; Glarborg, P. *Proc Combust Inst* **2015**, *35*, 553–560.

(69) Rasmussen, C. L.; Glarborg, P. *Combust Flame* **2008**, *154*, 529–545.

(70) Tian, Z.; Li, Y.; Zhang, L.; Glarborg, P.; Qi, F. *Combust Flame* **2009**, *156*, 1413–1426.

(71) Mendiara, T.; Glarborg, P. *Combust Flame* **2009**, *156*, 1937–1949.

(72) Mendiara, T.; Glarborg, P. *Energy Fuels* **2009**, *23*, 3565–3572.

(73) Klippenstein, S. J.; Harding, L. B.; Glarborg, P.; Miller, J. A. *Combust Flame* **2011**, *158*, 774–789.

(74) Abian, M.; Alzueta, M. U.; Glarborg, P. *Int J Chem Kinet* **2015**, *47*, 518–532.

(75) Song, Y.; Hashemi, H.; Christensen, J. M.; Zou, C.; Marshall, P.; Glarborg, P. *Fuel* **2016**, *181*, 358–365.

(76) Talbi, D.; Ellinger, Y. *Chem Phys Lett* **1998**, *288*, 155–164.

(77) Hansel, A.; Scheiring, C.; Giantschnig, M.; Lindinger, W.; Ferguson, E. E. *J Chem Phys* **1998**, *109*, 1748–1750.

(78) Goos, E.; Burcat, A.; ; Ruscic, B. *Ideal gas thermochemical database with updates from active thermochemical tables*; (<ftp://ftp. technion. ac. il/pub/supported/aetdd/-thermodynamics> mirrored at <http://garfield. chem. elte. hu/burcat/burcat. html>, 2013, 2016.

(79) Ruscic, B.; Pinzon, R. E.; Morton, M. L.; von Laszewski, G.; Bittner, S.; Nijsure, S. G.; Amin, K. A.; Minkoff, M.; Wagner, A. F. *J Phys Chem A* **2004**, *108*, 9979–9997.

(80) Ruscic, B.; Pinzon, R. E.; von Laszewski, G.; Kodeboyina, D.; Burcat, A.; Leahy, D.; Montoya, D.; Wagner, A. F. *J Phys Conf Ser* **2005**, *16*, 561–570.

(81) Tsang, W.; Herron, J. T. *J Phys Chem Ref Data* **1991**, *20*, 609–663.

(82) Baulch, D. L.; Bowman, C. T.; Cobos, C. J.; Cox, R. A.; Just, T.; Kerr, J. A.; Pilling, M. J.; Stocker, D.; Troe, J.; Tsang, W.; Walker, R. W.; Warnatz, J. *J Phys Chem Ref Data* **2005**, *34*, 757–1397.

(83) Wooldridge, S. T.; Hanson, R. K.; Bowman, C. T. *Int J Chem Kinet* **1995**, *27*, 1075–1087.

(84) Miller, J. A.; Melius, C. F. *Proc Combust Inst* **1986**, *21*, 919–927.

(85) Sumathi, R.; Nguyen, M. T. *J Phys Chem A* **1998**, *102*, 8013–8020.

(86) Bunkan, A. J. C.; Tang, Y.; Sellevag, S. R.; Nielsen, C. J. *J Phys Chem A* **2014**, *118*, 5279–5288.

(87) Jiang, B.; Guoa, H. *J Chem Phys* **2013**, *139*, 224310.

(88) Montgomery, J., J. A.; Frisch, M. J.; Ochterski, J. W.; Petersson, G. A. *J Chem Phys* **1999**, *110*, 2822–2827.

(89) Frisch, M. J. et al. *Gaussian 09*; 2000.

(90) Jacobs, A.; Wahl, M.; Weller, R.; Wolfrum, J. *Chem Phys Lett* **1988**, *144*, 203–207.

(91) Higashihara,; T.,; Saito,; K.,; Murakami,; I., *J Phys Chem* **1983**, *87*, 3707–3712.

(92) Dagaut, P.; Lecomte, F.; Chevailler, S.; Cathonnet, M. *Combust Sci Technol* **2000**, *155*, 105–127.

Table 1: Values reported in literature for the thermodynamic properties of HNC (heat of formation of HNC and the energy difference between HNC and HCN).

ΔH^0_{f298}(HNC) - ΔH^0_{f298}(HCN) kcal mol^{-1}	ΔH^0_{f298}(HNC) kcal mol^{-1}	Method	Ref.
14.6	45.5[a]	Theory	[15]
15.0±2	45.9±2[a]	Theory	[20]
10.3±1.1	41.2±1.1[a]	Exptl.	[22]
>17	>47.9[a]	Exptl.	[23]
14.8±2	45.7±2[a]	Exptl.	[24]
14.4±1	45.3±1[a]	Theory	[32]
12.9	43.8[a]	Theory	[10]
14.7	45.6	Theory	[34]
15.2	46.1[a]	Theory	[35]
15.2	46.1[a]	Theory	[38]
13.8	44.7[a]	Theory	[76]
14.4	45.3±1[a]	Exptl.	[42]
14.0±1[b]	44.9±1	Exptl.	[77]
18.8±2.9[b]	49.7±2.9	Exptl.	[45]
14.7±0.14	45.6±0.14[a]	Theory	[46]
14.2	45.1[a]	Theory	[52]
16.3	47.2[a]	Exptl, theory	[61]
14.2	45.1[a]	Theory	[62]
15.07	45.95±0.09	Theory, ATcT	[67]

a: Estimated from ΔH^0_{f298}(HNC) - ΔH^0_{f298}(HCN), assuming ΔH^0_{f298}(HCN) = 30.9 kcal mol^{-1}.[67]
b: Estimated from ΔH^0_{f298}(HNC), assuming ΔH^0_{f298}(HCN) = 30.9 kcal mol^{-1}.[67]

Table 2: Thermodynamic properties of selected species in the reaction mechanism. Units are kcal mol^{-1} for H, and cal mol^{-1} K^{-1} for S and C_p. Temperatures are in K. Data are drawn from the thermodynamic database of Goos, Burcat and Ruscic[78], except that the heat of formation of HNC was updated according to the work of Nguyen et al.[67].

Species	H_{298}	S_{298}	$C_{p,300}$	$C_{p,400}$	$C_{p,500}$	$C_{p,600}$	$C_{p,800}$	$C_{p,1000}$	$C_{p,1500}$
HCN	31.02	48.23	8.59	9.36	9.97	10.48	11.31	12.01	13.20
HNC	45.95	49.11	9.64	10.22	10.61	10.92	11.55	12.08	13.09
CN	105.15	48.42	6.97	7.04	7.16	7.32	7.69	7.99	8.48

Table 3: Selected reactions important for prompt NO formation. Parameters for use in the modified Arrhenius expression k=AT^{β}exp(-E/[RT]). Units are mol, cm, s, cal.

		A	β	E_a	Source
1.	$HCN + M \rightleftharpoons CN + H + M^a$	3.4E35	-5.130	133000	[81]
	$HCN + N_2 \rightleftharpoons CN + H + N_2$	3.6E26	-2.600	124890	
2.	$HCN + M \rightleftharpoons HNC + M^b$	1.6E26	-3.230	51840	[11], *c*
3.	$CN + H_2 \rightleftharpoons HCN + H$	1.1E05	2.600	51908	[82]
4.	$HCN + O \rightleftharpoons NCO + H$	1.4E04	2.640	4980	[1]
5.	$HCN + O \rightleftharpoons NH + CO$	3.5E03	2.640	4980	[1]
6.	$HCN + O \rightleftharpoons CN + OH$	4.2E10	0.400	20665	[11]
7.	$HCN + OH \rightleftharpoons CN + H_2O$	3.9E06	1.830	10300	[83]
8.	$HCN + OH \rightleftharpoons HOCN + H$	5.9E04	2.430	12500	[84]
9.	$HCN + OH \rightleftharpoons HNCO + H$	2.0E-03	4.000	1000	[84]
10.	$HCN + OH \rightleftharpoons NH_2 + CO$	7.8E-04	4.000	4000	[84]
11.	$HCN + O_2 \rightleftharpoons CN + HO_2$	3.0E13	0.000	75100	[9] est
12.	$HNC + H \rightleftharpoons HCN + H$	7.8E13	0.000	3600	[85]
13.	$HNC + O \rightleftharpoons NH + CO$	4.6E12	0.000	2200	[11]
14.	$HNC + OH \rightleftharpoons HNCO + H$	3.6E12	0.000	-479	[86], *d*
15.	$HNC + OH \rightleftharpoons CN + H_2O$	3.0E02	3.160	10600	pw
16.	$HNC + O_2 \rightarrow$ products		slow		pw, *e*

a: Third body efficiencies: N_2=0, O_2=1.5, H_2O=10

b: Third body efficiencies: Ar=0.7, H_2O=7, CO_2=2

c: The activation energy was modified according to the updated heat of formation of HNC.

d: Arrhenius expression fitted from data in the reference.

e: The HNC + O_2 reaction has a calculated barrier of 44 kcal mol^{-1} and was not included in the modeling.

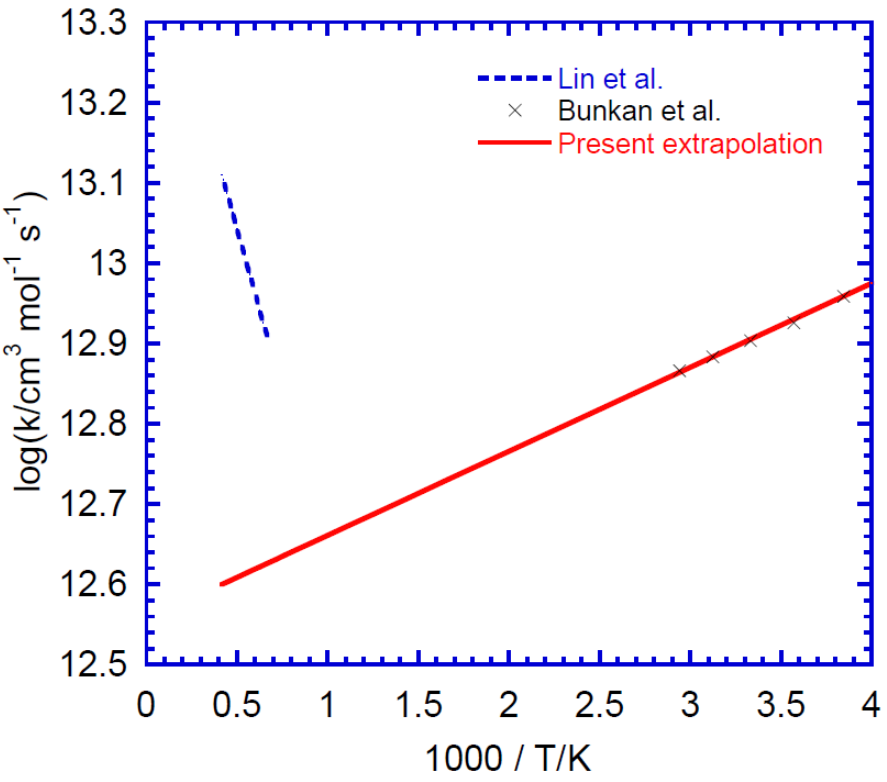

Figure 1: Arrhenius plot for the reaction HNC + OH $\rightleftharpoons$ HNCO + H. The symbols denote high level theory data from Bunkan et al.[86] while the dashed line denotes the rate constant calculated by Lin et al.[10]. The solid line is our extrapolation of the data of Bunkan et al. to relevant temperatures.

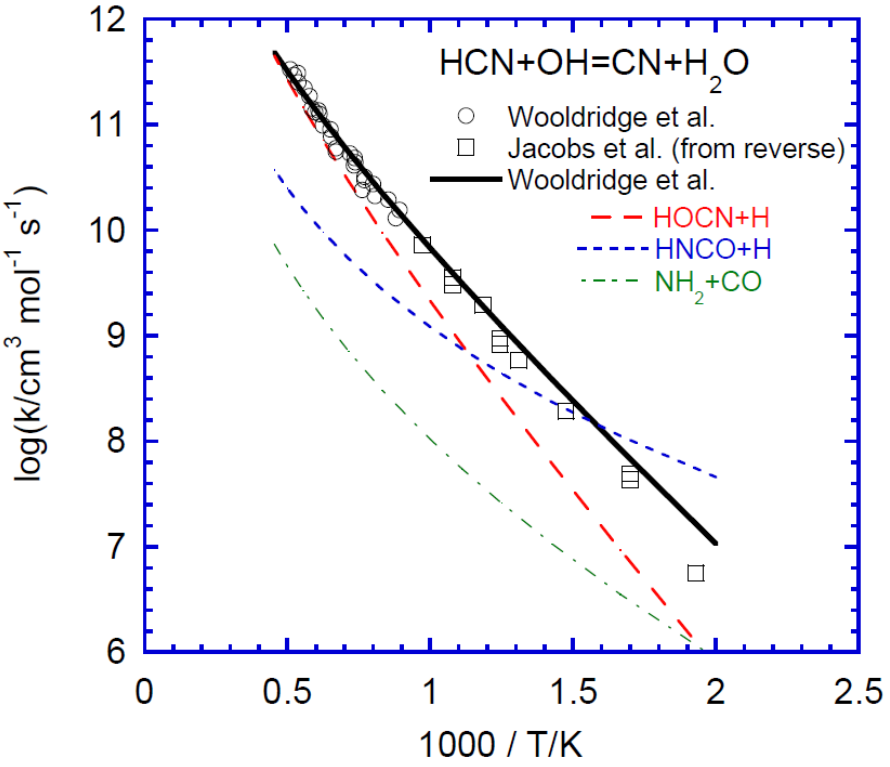

Figure 2: Arrhenius plot for the reaction HCN + OH ⇌ CN + H_2O (R7). The symbols denote experimental results from Wooldridge et al.[83] and from Jacobs et al.[90] (from measurements of CN + H_2O, reversed through the equilibrium constant) while the solid line shows the constant recommended by Wooldridge et al. Also shown (dashed lines) are rate constants for the secondary channels to HOCN + H (R8), HNCO + H (R9), and NH_2 + CO (R10), drawn from BAC-MP4 calculations by Miller and Melius[84].

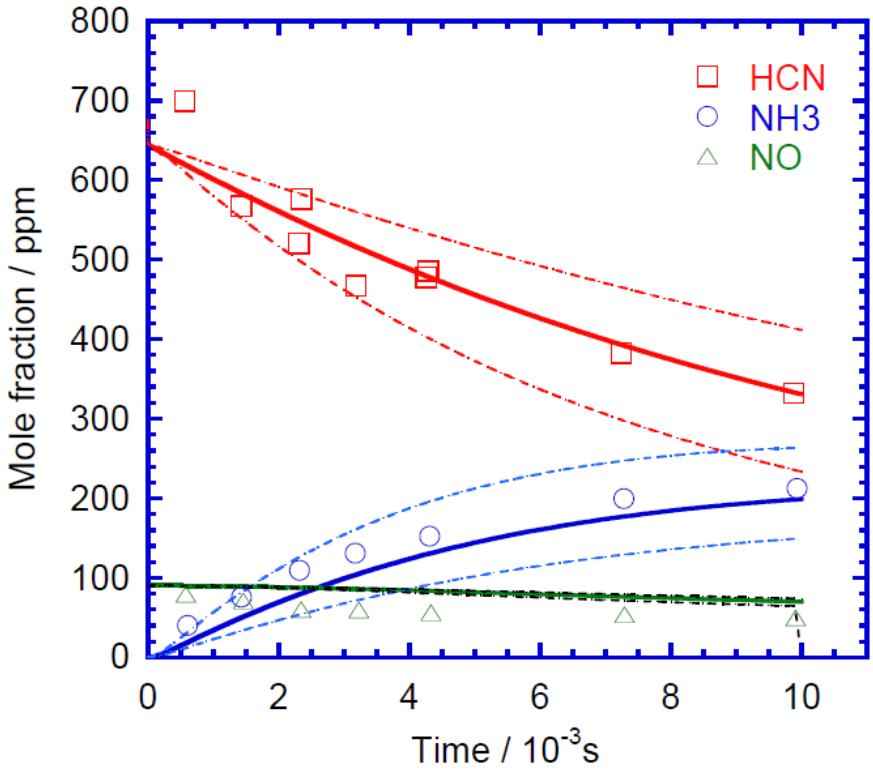

Figure 3: Comparison between experimental data[8] and modeling predictions for HCN oxidation in the post-flame region of an atmospheric pressure, premixed, fuel-rich ethylene-air flame doped with 680 ppm ammonia. Fuel-rich equivalence ratio $\phi = 1.66$; temperature 2000 K. Symbols denote experimental data while lines denote model predictions. Solid lines denote predictions with the present model while dashed lines show the effect of varying the rate constant k_{14} for HNC + OH by a factor of two.

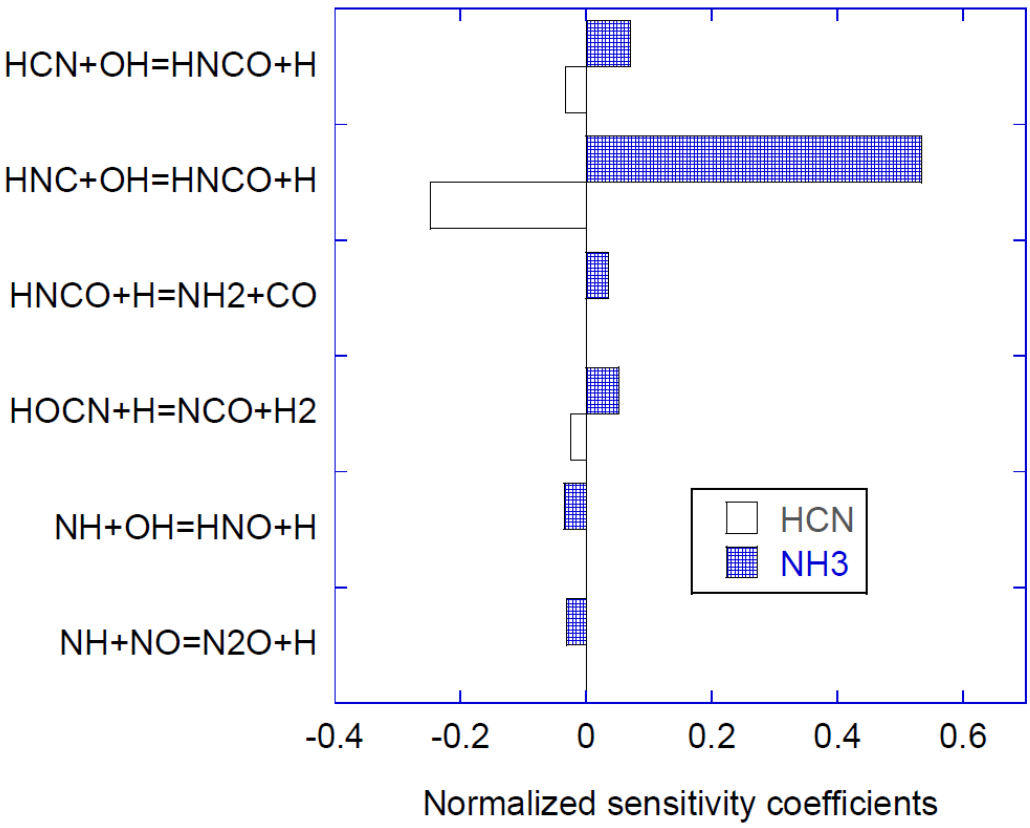

Figure 4: First order sensitivity coefficients for HCN and NH_3 for the conditions of the flame in Fig. 3.

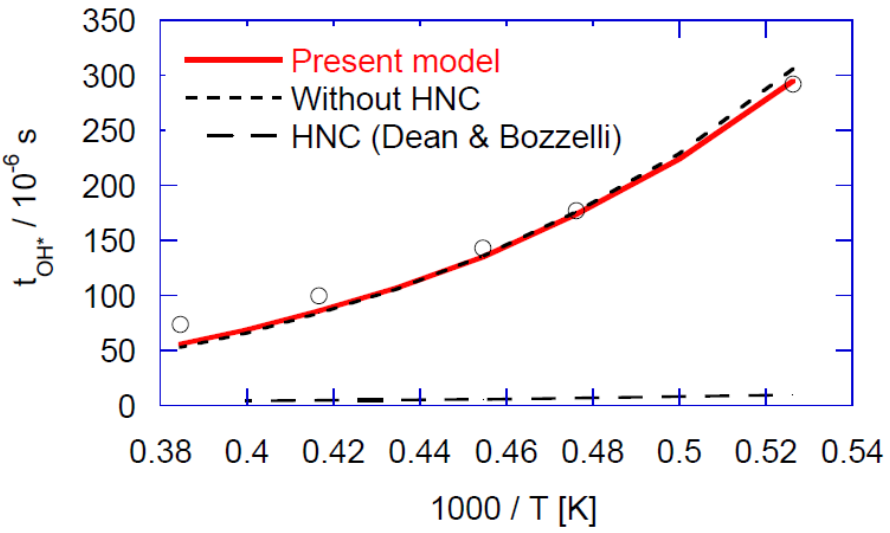

Figure 5: Comparison between measured[91] and predicted induction times as a function of temperature for oxidation of HCN (1%) by O_2 (1%) in argon in a shock tube. The experimental data are derived from the least-squares analysis expression by Higashihara et al., assuming P = 1.0 atm. In the calculations the induction time is taken as the time to reach 25% of the peak concentration for O. Experimental data are shown as symbols, while modeling predictions are shown as lines.

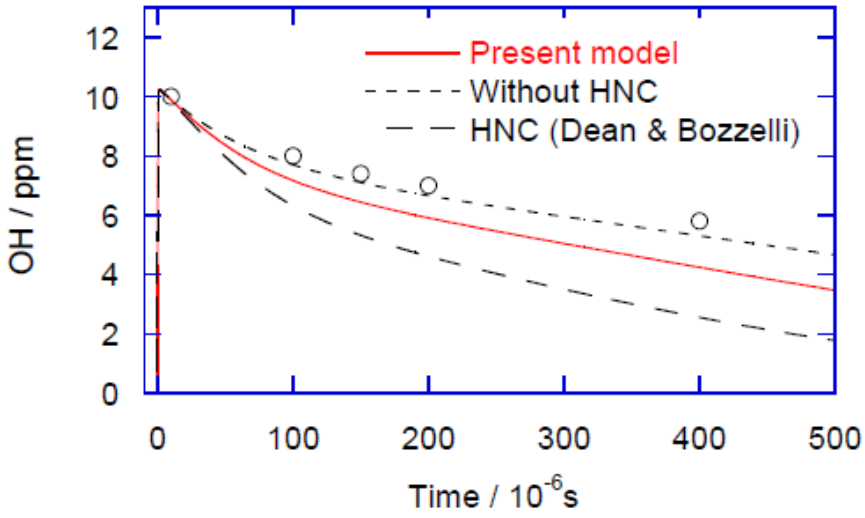

Figure 6: Comparison between measured[83] and predicted OH absorption traces from the reflected shock pyrolysis of 10.3 ppm HNO_3, 0.34% HCN in argon for T = 1492K and P = 1.01 atm. Experimental data are shown as symbols, while modeling predictions are shown as lines.

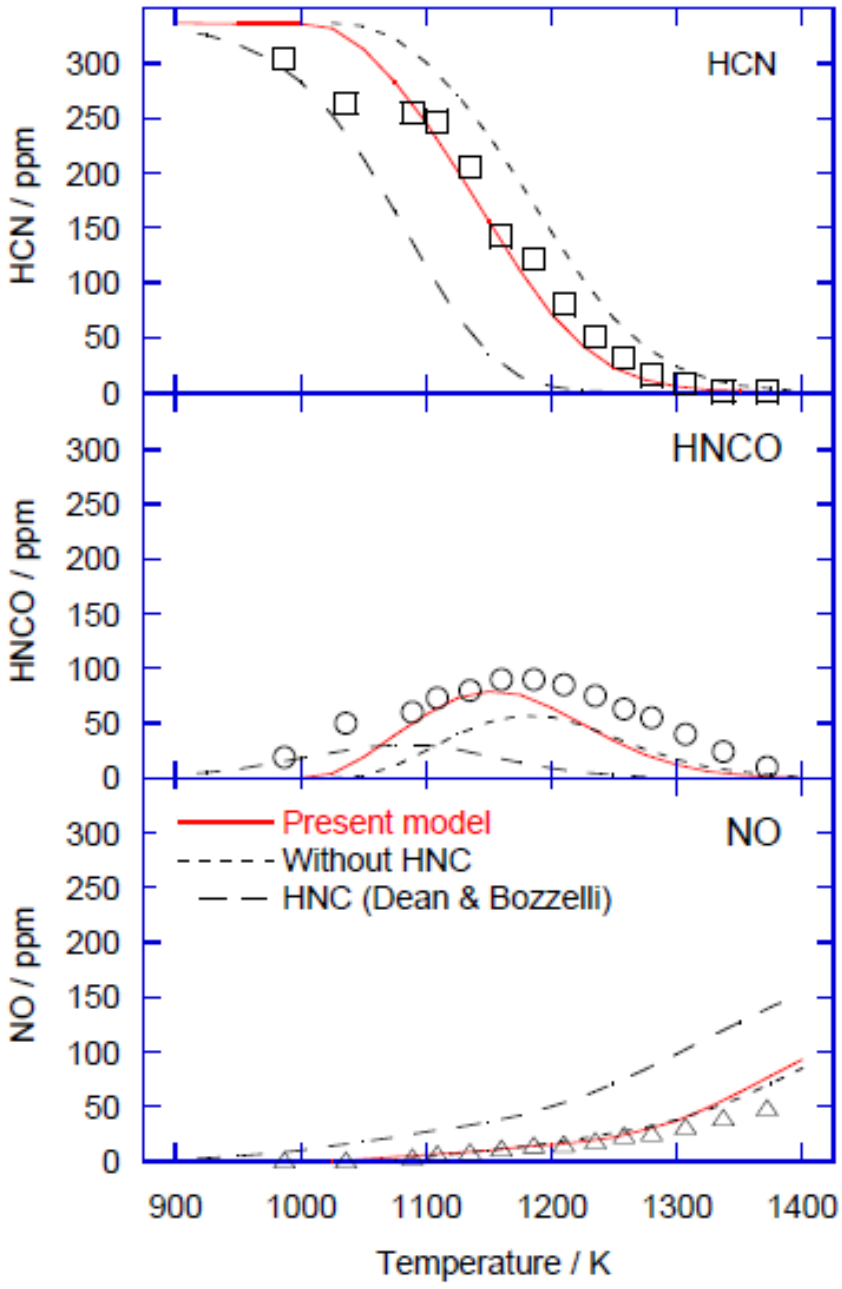

Figure 7: Comparison between experimental data[13] and modeling predictions for HCN oxidation in a flow reactor. Symbols denote experimental data while lines denote model predictions. Inlet concentrations: 337 ppm HCN, 2.6% O_2, 3.1% H_2O; balance N_2. Pressure is 1.05 atm. Residence time at 1200 K (constant constant mass flow) is 112 ms.

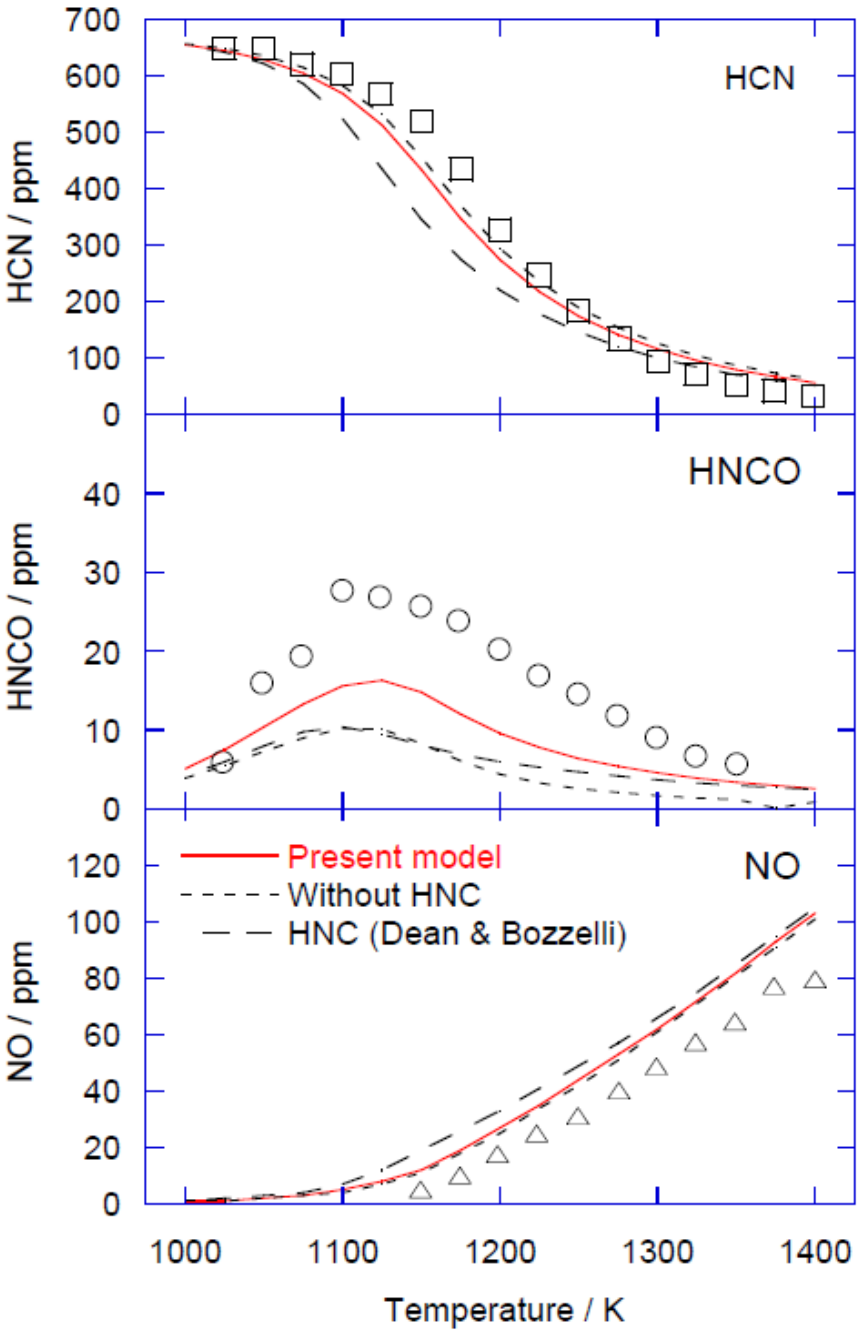

Figure 8: Comparison between experimental data[92] and modeling predictions for HCN oxidation in a jet-stirred reactor. Symbols denote experimental data while lines denote model predictions. Inlet concentrations: 670 ppm HCN, 2000 ppm O_2, 200 ppm H_2O; balance N_2. Pressure is 1.0 atm. Residence time 120 ms.